Wind Engineering Joint Usage/Research Center
FY2021 Research Result Report

Research Field: Indoor Environment
Research Year: FY2021
Research Number: 20212012
Research Theme: Research on prediction method of indoor temperature distribution based on Contribution Ratio of Indoor Climate (CRI) and mobile sensor information

Representative Researcher: Weirong Zhang

Budget [FY2021]: 400000Yen

*There is no limitation of the number of pages of this report.
*Figures can be included to the report and they can also be colored.
*Submitted reports will be uploaded to the JURC Homepage.

1. Research Aim

With the increasing requirements of satisfying individual thermal comfort and improving building energy efficiency, the indoor temperature distribution has been attracted more and more attention. Generally, we use Computational Fluid Dynamics (CFD) to obtain the temperature distribution. However, it has the limitation of long calculation time and high calculation load. Additionally, when the thermal boundary conditions change, it is necessary to start repeated calculation. Under this condition, a prediction method of indoor temperature distribution based on the fixed sensor data and the Contribution Ratio of Indoor Climate (CRI) has been proposed. The CRI is an effective index to evaluate the independent contribution of each heat source to temperature distribution. However, the CRI fixed value hypothesis limits its application in practical situations and due to the limitation of the fixed sensors in both installation location and installation number, the prediction accuracy needs to be improved.
The aim of this study is to proposed a fast prediction method for indoor temperature distribution without knowing the thermal boundary conditions in practical applications and to introduce interpolation POD (proper orthogonal decomposition) method to obtain the dynamic distribution of CRI. Based on a typical office model, the effectiveness of using mobile sensors was discussed, and the influence of its acquisition height and acquisition distance on the prediction accuracy was analyzed as well. As a case study, in a simplified office model with identified heat source conditions, based on the interpolation POD method, the reconstruction of each sub temperature field dominated by only one heat source under any air supply parameters was realized, and thus its CRI distribution could be calculated. The effectiveness of POD method breaks the application limitations of CRI fixed value hypothesis on the proposed method, and further promotes its development potential in the direction of "real-time prediction and dynamic regulation" in practical application.

2. Research Method

2.1 Prediction algorithm based on Contribution Ratio of Indoor Climate (CRI)

2.1.1 Contribution Ratio of Indoor Climate (CRI)

Generally, the construction of indoor airflow field is affected by both forced convection and natural convection. When there is a forced air supply in the room, due to the influence from the heat sources is smaller than that of air supply and thus can be ignored, the airflow field is usually considered as being dominated by the forced convection. On this condition, when the velocity and temperature of air supply are constant, the airflow field can be considered as steady-state, even if the influence caused by the small-scale change of heat source intensity exist.

Therefore, in a steady-state airflow field, the temperature field can be assumed as linear. That is, the indoor temperature field can be regarded as the superposition of all sub-temperature fields dominated by only one heat source. To indicate the range and degree of influence from each heat source within steady airflow field, so as to estimate its independent contribution to the indoor temperature distribution, an index named Contribution Ratio of Indoor Climate (CRI) extracted from CFD calculation results was proposed. In a forced convection airflow field, it is defined as the ratio of temperature rise or drop at a location caused by each heat source to the absolute value of uniform temperature rise or drop caused by the same heat source. Its value is a relative intensity, in which the actual temperature rise/drop caused by each heat source is normalized by the absolute value of its own perfect mixing condition. For example, a CRI higher/lower than 1.0 at a location means that the influence of that heat source is higher/smaller than that in the case of perfect mixing. The CRI of the heat source i at the location X_j was defined by Equation (1),

$$CRI_i(X_j) = \frac{\theta_i(X_j) - \theta_n}{(q_i / C_p \rho F)} \tag{1}$$

Where $\theta_i(X_j)[°C]$ is the air temperature at the location X_j caused by heat source i; $\theta_n[°C]$ is the air neutral temperature; $q_i[W]$ is the heat emission or absorption of heat source i; $C_p[J/(kg \cdot K)]$ is the specific heat of indoor air; $\rho[kg/m^3]$ is the air density; $F[m^3/s]$ is the volume of supply air.

Until now, the CRI has been applied in many applications, including the couple with network models and the prediction of indoor temperature distribution, and also has been extended to the response factor of heat sources in transient cases and the evaluation of contaminant and moisture distribution. In the previous study of researchers, CRI theoretical system has also been comprehensively and systematically established, including its basic premises, definitions, calculation methods and mathematical meaning.

2.1.2 Prediction algorithm

The linear assumption of temperature field in steady airflow field means that the heat transfer of each heat source in the space changes linearly with the heat source intensity, the CRI of each heat source thus is a fixed value. Accordingly, a method using CRI and finite air temperature collected by fixed sensors to predict indoor temperature distribution has been proposed []. Due to the limitation of fixed sensors in installation number and installation location, researchers have proposed using mobile sensors instead of fixed sensors to collect air temperature to improve the prediction accuracy []. The temperature rise or drop from θ_n at the location X_j can be expressed by Equation (2),

$$\Delta\theta(X_j) = \begin{bmatrix} C_{j1} & C_{j2} & \cdots & C_{jm} \end{bmatrix} \begin{bmatrix} C_{11} & C_{12} & \cdots & C_{1m} \\ C_{21} & C_{22} & \cdots & C_{2m} \\ \vdots & \vdots & \ddots & \vdots \\ C_{1m} & C_{2m} & \cdots & C_{mm} \end{bmatrix}^{-1} \begin{bmatrix} \Delta\theta'_{s1} \\ \Delta\theta'_{s2} \\ \vdots \\ \Delta\theta'_{sn} \end{bmatrix} \tag{2}$$

Where $\Delta\theta(X_j)$ is the temperature rise or drop from θ_n at the location X_j; C_{ji} is the CRI of heat source i to location X_j; $\Delta\theta'_{si}$ is the temperature rise or drop collected by mobile sensors from θ_n;

Using this prediction algorithm can realize the rapid prediction of indoor temperature distribution.

In our previous study, it has been proposed to use mobile sensors instead of fixed sensors to collect air temperature substituted into the algorithm to improve the prediction accuracy. To further improve the applicability of this algorithm in the long-term calculation or dynamic calculation, it is necessary to obtain the dynamic distribution of CRI of each heat source according to the change of actual environment.

2.2 Mobile sensors

A method was proposed before using some fixed sensors equal to the number of heat sources to collect air temperature in space, and then combined them with CRI for

temperature distribution prediction. This method is suitable for practical applications without identified boundary conditions in advance. However, there are limitations in terms of both installation location and installation number. For example, when the number of monitored data increases, the number of fixed sensors also needs to increase, leading to higher expense and bigger installation space. Additionally, the installation location of fixed sensors is not changeable and is usually far away from the target control area, such as near air outlets, high position on the wall or where people are not easy to touch. This means that the air temperature collected is location-dependent, so may not be representative to the real situation of each heat source.

With the development of mobile carriers in control engineering, mobile sensors technology has become a popular solution for controlling buildings' indoor environment, to overcome the limitations of fixed sensors. These researches generally do not consider thermal factors, especially the influence of change in heat source on airflow field, and cannot achieve simple calculation of temperature at any location within a space. However, using mobile sensors to monitor environmental information provides a feasible and efficient idea for studies of indoor thermal environment.

Therefore, in this study, one mobile sensor (as shown in Figure 1) has been used to replace fixed sensors, when collecting air temperature within space. Mobile sensors have the characteristics of variable acquisition height, diverse acquisition path and flexible acquisition location. They are adjustable according to actual requirements or prediction demand to collect more suitable data with no restrictions, to achieve better temperature distribution prediction by Equation (2).

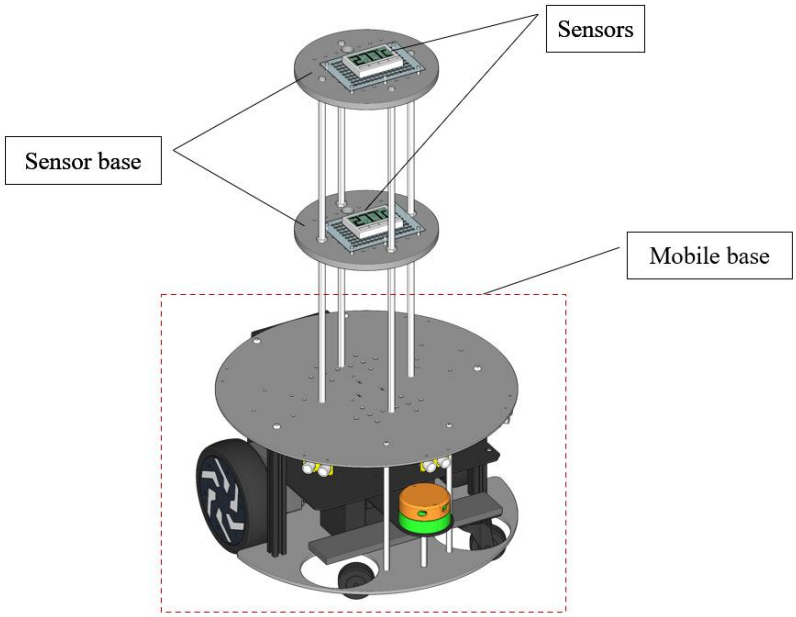

Fig.1. A mobile sensor

2.3 POD theory

The basic idea of POD method is that extracts a few representative modes in energy sense, which belongs to the category of projection methods. Specifically, it can help to project the original physical field onto finite modes to reduce the model order, and then reconstruct the physical field more easily. The detailed calculation procedure of POD is as follows:

(1) Built the target parameter matrix based on a series of snapshots,

$$\mathbf{S} = \left(\mathbf{s}^1 \quad \mathbf{s}^2 \quad \cdots \quad \mathbf{s}^N\right) \tag{3}$$

Where $\mathbf{s}^i$ is the distribution vector of physical field parameters in the ith snapshot; N is

the number of snapshots.

(2) Construct the auto covariance matrix of the target parameter matrix,

$$\mathbf{C} = \mathbf{S}^{\mathrm{T}}\mathbf{S} \tag{4}$$

(3) Solve the eigenvalues and eigenvectors of the auto covariance matrix,

$$\mathbf{CW} = \lambda\mathbf{W} \tag{5}$$

Where λ is the eigenvalues; $\mathbf{W}$ is the eigenvectors.

(4) Arrange the calculated eigenvalues in order from large to small,

$$\lambda_1 > \lambda_2 > \ldots > \lambda_N = 0 \tag{6}$$

The number of eigenvalues and eigenvectors is equal to the number of snapshots and corresponds one by one. The proportion of each eigenvalue to the sum of all eigenvalues reflects the physical field energy captured by the corresponding eigenvector, which is generalized energy. Generally, the number of eigenvalues that can capture 99% of the energy of the physical field is sufficient. Therefore, the required number of eigenvalues can be determined according to Equation (7),

$$\frac{\sum_{i=1}^{P}\lambda_i}{\sum_{j=1}^{N}\lambda_j} \geq 99.99\% \tag{7}$$

(5) Calculate the POD modes,

$$\boldsymbol{\varphi}^i = \frac{\sum_{n=1}^{P}\mathbf{A}_n^i\mathbf{s}^n}{\left\|\sum_{n=1}^{P}\mathbf{A}_n^i\mathbf{s}^n\right\|} \tag{8}$$

Where A_n^i is the ith order component of the eigenvector corresponding to the ith eigen value.

(6) Calculate the mode coefficient corresponding to each POD mode,

$$\mathbf{a}^n = \left[\boldsymbol{\varphi}^1 \quad \boldsymbol{\varphi}^2 \quad \cdots \quad \boldsymbol{\varphi}^n\right]^T \mathbf{s}^n \tag{9}$$

(7) Reconstruct the physical field according to Equation (9).

3. Research Result

3.1 Verification of the prediction algorithm based on experiments

In order to obtain the real room temperature distribution, in-depth study of the influence of heat sources on the temperature field, and to verify the follow-up simulation results, a three-day experiment was carried out in an office room in Beijing University of Technology (from November 2, 2021 to November 4, 2021), the specific layout is shown in Figure 2a.

Under the non-uniform room temperature environment created by each heat source and air conditioner, the temperature at different heights is measured by fixing thermocouples with 10 vertical rods, so as to obtain the temperature value of each measuring point. In addition, four hot-wire anemometers are fixed to measure the magnitude of the north wind in the horizontal direction for comprehensive verification of the temperature field and velocity field. The curtains were closed during the experiment to reduce the influence of solar radiation (the windows of the experimental room face north, no direct sunlight). A total of 37 temperature measurement points were arranged in this experiment, including the temperature of different heights in the indoor space (fixed by vertical poles), wall temperature, air-conditioning outlet temperature and outdoor temperature (monitored by temperature and humidity self-meter); 4 speed measurement points were arranged, which passed the Change the calorific value and location of the heat source to design different

working conditions, in which only one working condition is involved in a day. Experiments were carried out indoors without people to reduce the disturbance of temperature caused by personnel activities.

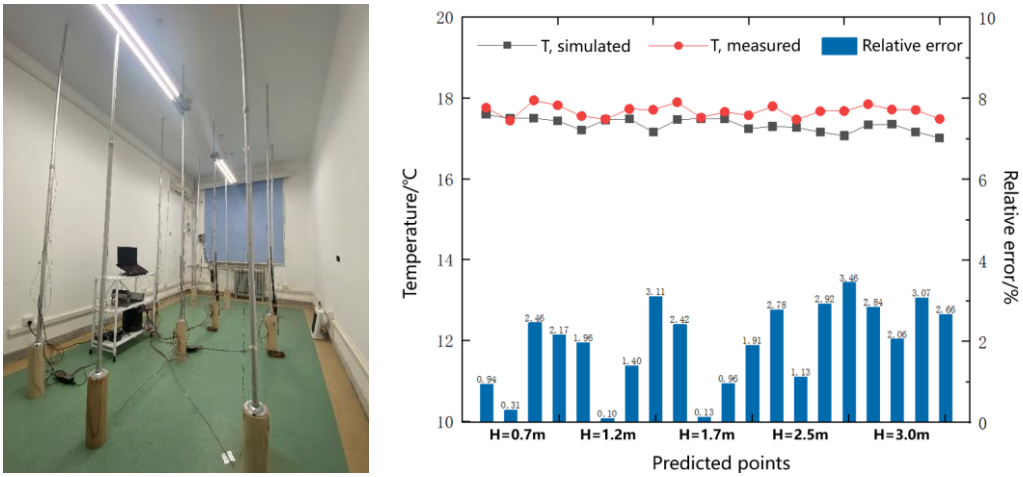

(a) an office room (b) Temperature comparison between simulation and experiment

Fig.2. The experiment room and temperature comparison

Compare the simulation and experimental results by building the same model as the experimental room (Figure 2b.). Through the simulation, the temperature value and wind speed value of the simulation result and the experimental result are compared, and the error result is found to be 1.9%. It is considered that the simulation result is correct within the allowable error range. It also provides real data support for subsequent simulation work.

Through experiments, temperature and wind speed data were obtained for a period of 3 days. After data analysis, it is found that firstly there is a temperature difference of 1-2 °C in different indoor spaces. The experimental conditions are reasonable and meet the experimental requirements. Secondly, after the curtains are drawn, the indoor temperature changes regularly with time, and is basically free from outdoor temperature fluctuations. Therefore, during this experiment, the curtains are conducive to creating a stable external environment, resulting in little correlation between the daily results and time, that is, the requirements for the experiment time are compared. Loose. Thirdly, the temperature trend of each point in the indoor space on different days is similar (the influencing factor may be the heat source disturbance), when the heat source position is the same, the trend is closer. Fourthly, temperature and wind speed at each measuring point show that the air outlet has a greater impact, and the impact on the measuring point is greater, which may be related to the small calorific value and low location of the heat source.

In order to obtain more quantitative and more convincing results, we continue to carry out experiments in a climate chamber, as can be seen from Figure 3. The climate chamber was constructed to systematically analyze the relationship between the natural crosswind fluctuations, the amount of sweat produced, and the skin temperature. It has a dimension of 5m wide×11m long×3m high. It houses a laboratory (3.7m wide×8m long×2.7m high), a pre-room and a fan room. Equipped with a heat source system and two compact air-conditioning units, it can provide the ideal temperature field with temperature differences.

In this experiment, two heat source intensities are set with 500W and 1000W. Different wind speed values are set under each heat source intensity. At the same time, five supply air temperatures of 20℃ 22℃ 24℃ 26℃ 28℃ are set. In this experiment, 36 temperature collection points and 7 wind speed collection points were arranged. A total of 35 working conditions was conducted so that we can obtain a large number of experimental data. By screening and analyzing the data, the correctness of the simulation is further verified while discovering the room temperature distribution

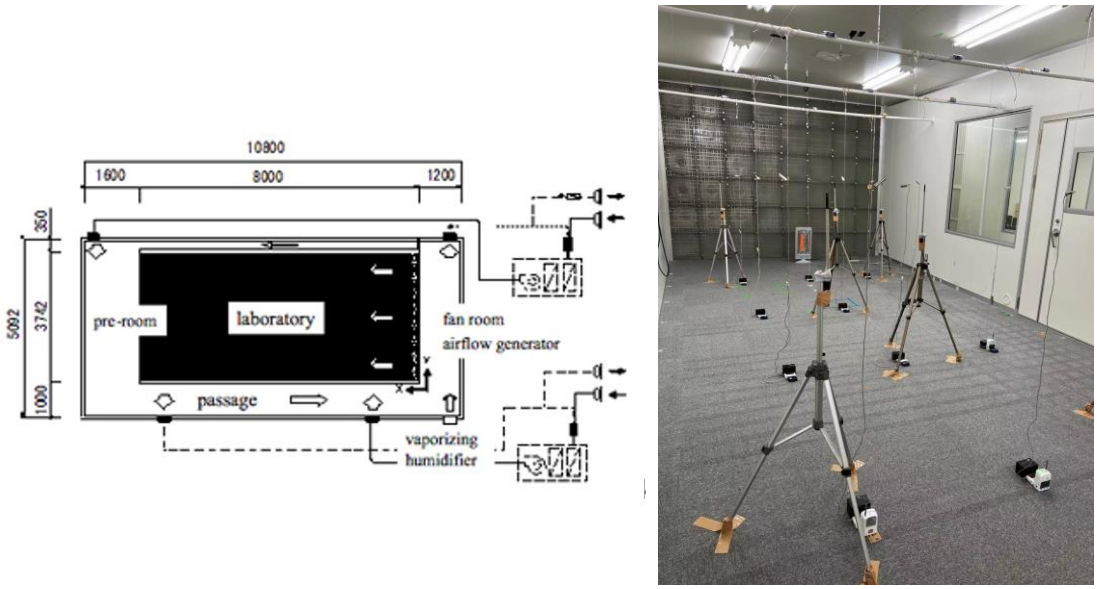

Fig.3. The climate chamber

3.2 Predicting indoor temperature distribution based on CRI and mobile sensors

As shown in Figure 4, a typical office model has been established in this study, with a dimension of 14m (length)×10m (width)×4m (height). There were four air supply inlets on the ceiling and four air exhaust outlets at the bottom of the two opposite walls. The walls, the ceiling and the floor of this office were all thermally insulated. There were 6 lamps and 24 working positions (each with a person and a computer) in the office. To simplify the computational model, the radiative heat transfer of walls and floor were considered as one heat source. Similarly, the radiative heat transfer of ceiling and the heat emission from 6 lamps were considered as one heat source. This left the heat emission from 4 adjacent working positions, which were considered as one heat source. Therefore, there were a total of 9 heat sources in this simulation work. The numerical method for calculating the temperature distribution of this office has been described above and the specific boundary conditions are listed in Table 1. The neutral temperature in the office was assumed to be 25°C. The office was discretized into 5,800,535, 7,784,596 and 10,746,488 hexahedral control volumes. After a grid-independence test, the middle definition was adopted to balance accuracy and time.

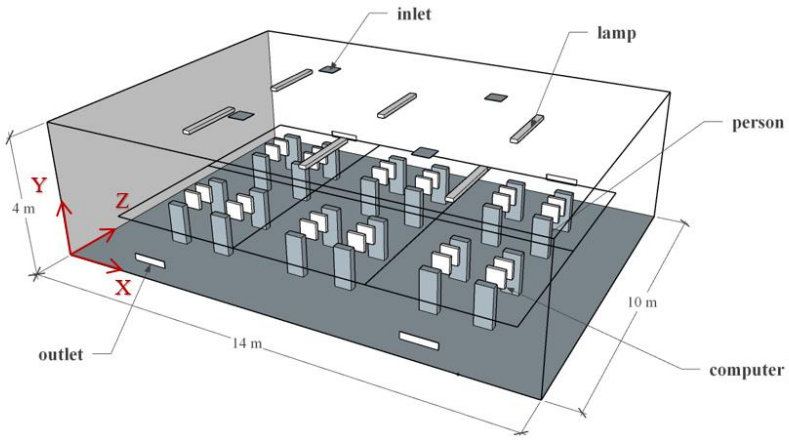

Fig. 4. A model for the office

Table 1. Summary of numerical simulation conditions

Surface	Boundary condition
Walls/Ceiling/Floor	Wall; Adiabatic.
Lamp	Wall; Heat flux: 150W/m².
Person	Wall; Heat flux: 45W/m².
Computer	Wall; Heat flux: 70W/m².
Air supply	Velocity-inlet; Velocity: 1.0m/s. Temperature: 21℃
Air exhaust	Outflow.

3.2.1 Comparison on prediction accuracy between fixed sensors and mobile sensors

In the comparison, 10 temperature prediction points in the plane with the height of 1m, 2m and 3m, respectively, have been selected. They were named as L-1 to L-10, M-1 to M-10 and H-1 to H-10, respectively. It should be noted that in this study, the locations of all prediction points were only different in height, but with identical plane coordinates. According to the requirements of the prediction algorithm, the number of collected air temperature needs to be equal to the number of heat sources. Nine air temperatures were collected. Given a group of fixed sensors location as shown in Figure 5. It is worth noting that the acquisition location of the sensors has a great impact on the prediction results. In other words, even if the number of sensors is the same, different results and prediction accuracy will be obtained by using the proposed algorithm due to different acquisition locations. For example, when the fixed sensors were installed near each heat source, respectively, the prediction accuracy was acceptable. While there are two reasons why fixed sensors were all installed on the walls in this study: 1) This is more suitable for the actual situations; 2) The purpose of this study is to verify the application disadvantages of fixed sensors. That is, taking the actual situations as references, the limitations of fixed sensors are analyzed and further the solutions are proposed. Meanwhile, a mobile sensor with the acquisition height of 1.2m was used to collect the air temperature of several locations in the space, also shown in Figure 5. The above two groups of collected air temperatures were used to predict the temperature of 30 points at the three heights, with their prediction results shown in Figure 6.

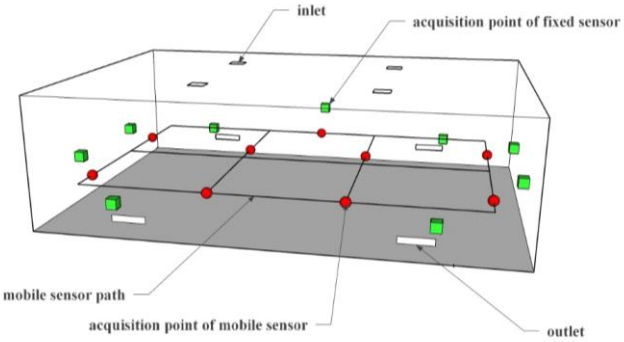

Fig. 5. Acquisition points of fixed sensors and mobile sensors

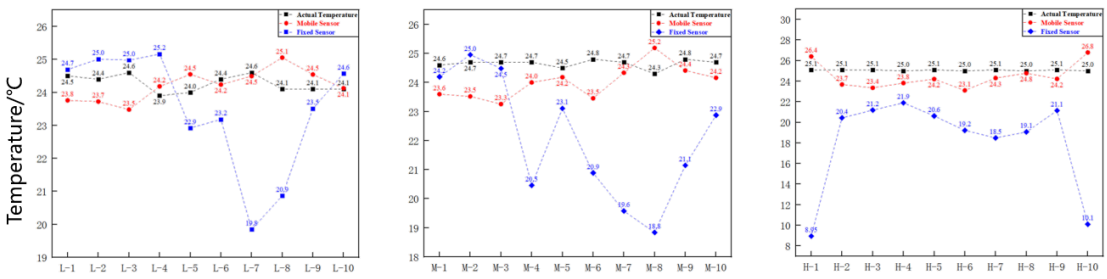

(a) h=1m (b)h=2m (c)h=3m

Fig. 6. Prediction of different heights using fixed sensors and mobile sensors

When the collected air temperature by fixed sensors was used for prediction, according to Table 2, the corresponding average relative errors were 5.7%, 10.8% and 27.7% at the heights of h=1.0m, h=2.0m and h=3.0m, respectively, which were relatively large.

Table 2. Prediction of each point using fixed sensors and mobile sensors

Average relative error	Fixed Sensors	Mobile Sensors
At the height of h=1.0m	5.7%	2.1%
At the height of h=2.0m	10.8%	3.3%
At the height of h=3.0m	27.7%	4.8%

Figure 6 showed that when using fixed sensors for temperature prediction, obvious abnormalities occurred at some locations, such as L-7 and L-8, H-1 and H-10. In addition to these reasons mentioned above, we assume their locations also have an impact on the prediction accuracy. L-7 and L-8 were located at the lower part of the room and closed to the supply air, which was more vulnerable to the influence of air backflow after the supply air meets the floor and other surfaces. Therefore, it will affect the CRI calculation of each heat source here and further affect the prediction accuracy. Similarly, H-1 and H-10 were located at the higher part and closed to the corner of the room. The airflow distribution here is affected by many factors, such as air backflow near the adjacent walls, heat plume above the heat source, etc. The prediction error thus also increases.

When using the mobile sensors with flexible acquisition location instead of the fixed sensors for temperature prediction, the corresponding average relative errors were 2.1%, 3.3% and 4.8%, respectively. On the one hand, this shows that the proposed temperature distribution prediction method based on CRI and finite air temperature is reliable. On the other hand, this indicates that due to some restrictions in practical applications, using mobile sensors instead of fixed sensors to predict the temperature distribution is appropriate. Besides, not in all cases, the prediction results obtained by using the mobile sensors are satisfactory.

3.2.2 Analysis on the impact of mobile sensors acquisition height on prediction accuracy

The height of the mobile sensor can be adjusted in the vertical direction according to the actual situation and the prediction demand. Generally, the regulation of indoor thermal environment is to reduce energy consumption but keeping satisfying indoor thermal environment. Therefore, the air temperature within human activity areas is usually the main controlled variable. To figure out the influence of the acquisition height of mobile sensors on the prediction accuracy of this area, 10 prediction points at the heights of h=0.7m, h=1.0m, h=1.2m and h=1.5m, named 1-P1 to 1-P10, 2-P1 to 2-P10, 3-P1 to 3-P10, 4-P1 to 4-P10 and 5-P1 to 5-P10, respectively, were selected, with identical plane coordinates, and used the air temperature obtained by the mobile sensor introduced in Section 4.1 to predict the air temperature at these points, with prediction results shown in Figure 7.

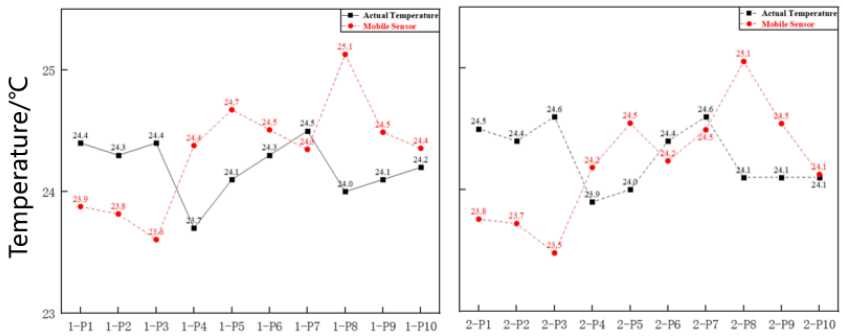

(a) h=0.7m (b) h=1.0m

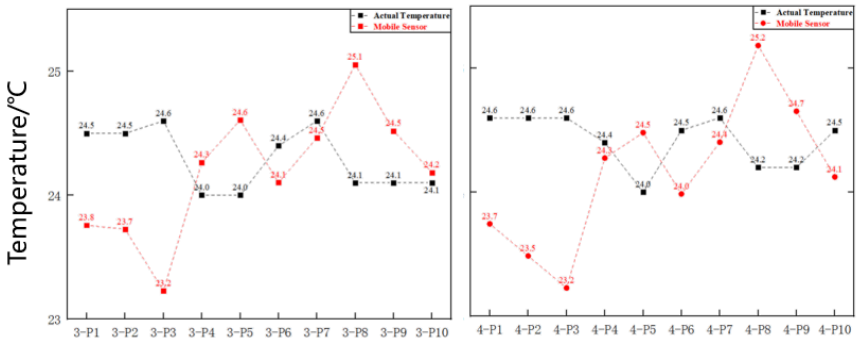

(c) h=1.2m (d) h=1.5m

Fig. 7. Prediction of different heights using mobile sensors

Table 3. Prediction of different heights using mobile sensors

Average relative error	Mobile Sensors
At the height of h=0.7m	2.1%
At the height of h=1.0m	2.1%
At the height of h=1.2m	2.3%
At the height of h=1.5m	2.7%

Similarly, according to Table 3, the corresponding average relative errors were 2.1%, 2.1%, 2.3% and 2.7% at the heights of h=0.7m, h=1.0m, h=1.2m and h=1.5m, respectively. Consequently, it can be concluded that in the human activity area, the acquisition height of mobile sensors has little influence on the prediction accuracy.

3.2.3 Analysis on the impact of mobile sensors acquisition distance on prediction accuracy

To better guide the application of mobile sensors in practical control, it should not only consider how to set the acquisition height of mobile sensors, but also consider the acquisition distance of mobile sensors. To explore the impact from this aspect, given mobile sensors acquisition path (the acquisition height was 1.2m), several acquisition distances were designed, which were 1m, 2m, 3m, 4m and 5m, respectively. In the case of each acquisition distance, 3, 3, 3, 3 and 2 acquisition point distributions were given, respectively, as shown in Figure 11 to Figure 15. The selected prediction points were the same as those at the 1.2m height discussed in Section 4.2, named 3-P1 to 3-P10.

Figure 8 and Table 4 also show the prediction results and the corresponding average relative errors of each prediction point under various distribution of acquisition points mentioned above, respectively. The prediction results showed that smaller acquisition distances would make the distribution of acquisition points more concentrated, hence leading to an obvious reduction in prediction accuracy. As shown in MS1, MS3, MS7 and MS10 in Figure 8, the corresponding average relative errors were 19.9%, 30.7%, 16.7% and 9.2%, respectively. However, it also had the situation that the prediction accuracy was relatively high with small acquisition distances, for example, the average relative errors were 1.6% and 0.8% in the cases of MS2 and MS6, respectively. This indicates that the uncertainty of temperature distribution prediction using the air temperature collected by mobile sensors with smaller acquisition distance was larger, and the prediction accuracy at this time cannot be guaranteed. When controlling indoor thermal environment in practical applications, it must quickly and accurately obtain temperature distribution. Therefore, it is necessary to give a design criterion for selecting an acquisition distance of mobile sensors with lower uncertainty, higher accuracy and wider application scope. Through a careful comparison of the prediction results under the distributions of acquisition points with various acquisition distances, as shown in Figure 8, a conclusion was drawn that the acquisition distance should be big enough to make the distribution of acquisition points more dispersed.

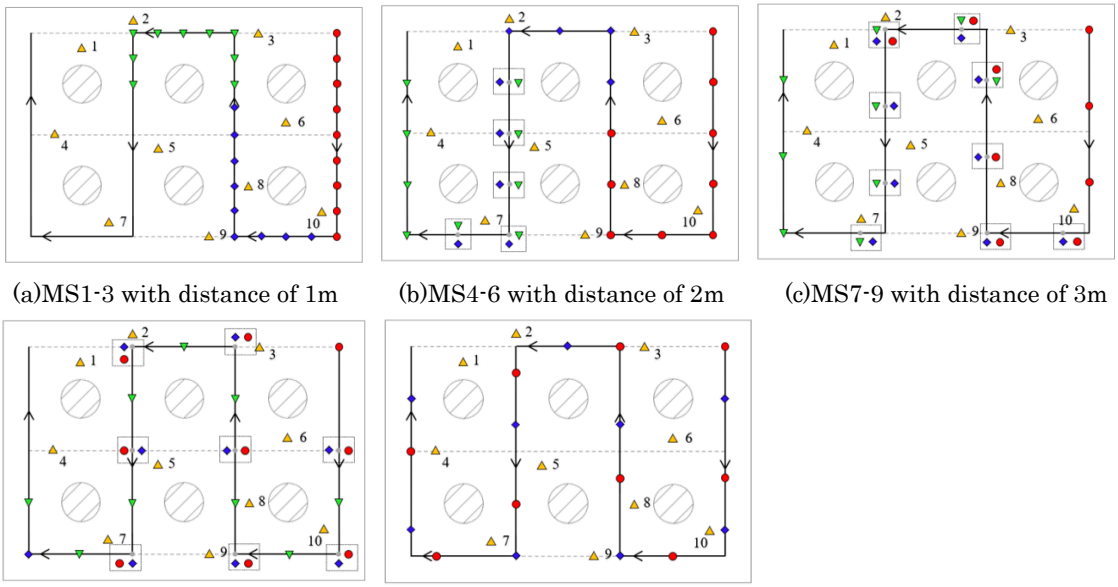

(a)MS1-3 with distance of 1m (b)MS4-6 with distance of 2m (c)MS7-9 with distance of 3m

(d)MS10-12 with distance of 4m (e)MS13-14 with distance of 5m

Fig. 8. Distributions of acquisition points with different acquisition distances

Table 4. Prediction of mobile sensors with different acquisition distance

	MS1	MS2	MS3	MS4	MS5	MS6
Average relative error	19.9%	1.6%	30.7%	2.7%	2.7%	0.8%
	MS7	**MS8**	**MS9**	**MS10**	**MS11**	**MS12**
Average relative error	16.7%	0.9%	1.4%	9.2%	0.5%	2.0%
	MS13	**MS14**				
Average relative error	2.1%	2.3%				

3.3 Approach on dynamic prediction of indoor temperature distribution by combing POD, CRI and mobile sensors

A hypothetical office model has been established in this study, with a dimension of 8m (length) × 5m (width) × 4m (height), as shown in Figure 9(a). Two air supply inlets (marked in red) and two air exhaust outlets (marked in blue) are located on the same side of the upper part of the room. The air supply direction is horizontal and the air exhaust direction is vertical. Built in two desks and eight work stations (Human heat flux: 45W/m^2), each station is equipped with a computer (Heat flux: 70W/m^2). After simplification, there are three heat sources in the office (people and computers located at two desks and air supply), as shown in Figure 9(b). Based on the proposed prediction algorithm, the number of air temperature collected by the mobile sensor is 3, which coordinates are A1 (4.0m, 1.0m, 2.0m), A2 (2.5m, 1.0m, 4.1m) and A3 (5.5m, 1.0m, 4.1m), as shown in Figure 9(b). Also, the plane y=1.0m is selected as the target plane. The neutral temperature is defined as 26℃. The numerical method used in this case is the same as the previous study, and its reliability has been verified. No more details here. After the verification of grid independence, the number of grids is 7,784,596 to balance the calculation accuracy and time. According to the adjustable range of air supply parameters, the interpolation interval of air supply speed and temperature was selected as 0.01m/s and 0.1℃ respectively, that is, there are 3321 air supply conditions in this case. The established sample database includes 9 air supply speeds (0.2m/s, 0.3m/s, 0.4m/s, 0.5m/s, 0.6m/s, 0.7m/s, 0.8m/s, 0.9m/s and 1.0m/s). Each speed corresponds to 3 air supply temperatures (20℃, 22℃ and 24℃), that is, there are 27 air supply conditions.

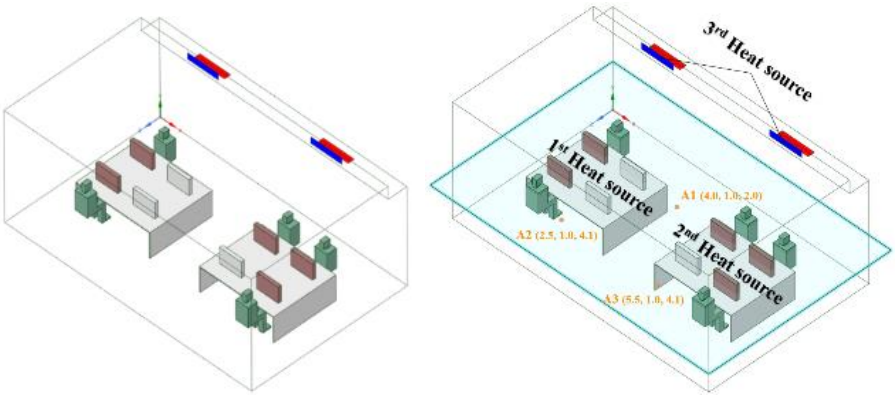

(a) (b)

Fig. 9. Room model and some detailed settings.

Firstly, the limitation of CRI fixed value hypothesis was verified. Taking the first group heat source as an example, when the air supply speed and temperature are v=0.3m/s and 24℃.When the air supply speed and temperature are v=0.9m/s and 22℃, CRI distributions at the two lines of x=4.0m and z=2.5m on the y=1.0m plane were shown in Figure 10.

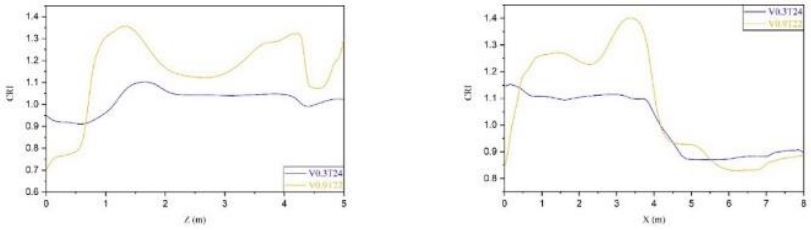

(a) line x=4.0m (b) line z=2.5m

Fig. 10. CRI comparison of first group heat source under two air supply conditions.

Through the analysis and comparison, when the air supply parameter change, the variation of CRI distribution cannot be ignored. Therefore, it is necessary to break the limitation brought by CRI fixed value hypothesis to improve the prediction accuracy.

Next is the calculation of POD mode and modal coefficients of various temperature fields. In this study, for the total temperature field and each sub temperature field, the first 3, first 1 and first 1 POD modes were selected for the reconstruction, which can cover almost all the data characteristics of the whole temperature field.

Then, according to the current air supply parameter conditions (T=23℃, v=0.45m/s), the total temperature distribution and each sub temperature distribution at target plane y=1.0m were reconstructed, as shown in Figure 11, Figure 12 and Figure 13 respectively. Correspondingly, the average relative error between the simulation results and reconstruction results are 0.58, 0.60 and 0.58. The detailed relative error analysis is shown in Figure 14(a), (b) and (c). It can be seen that the reconstruction results are reliable in most areas. While the relative error is relatively large in the areas with complex air distribution such as the vicinity of the heat source and the room boundary.

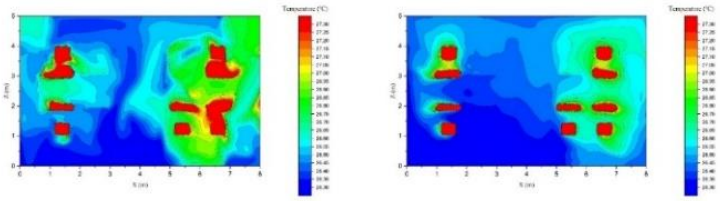

(a) CFD simulation (b) POD interpolation

Fig. 11. Total temperature distribution.

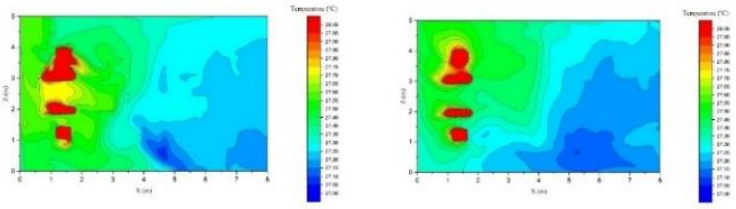

(a) CFD simulation (b) POD interpolation

Fig. 12. The first sub temperature distribution.

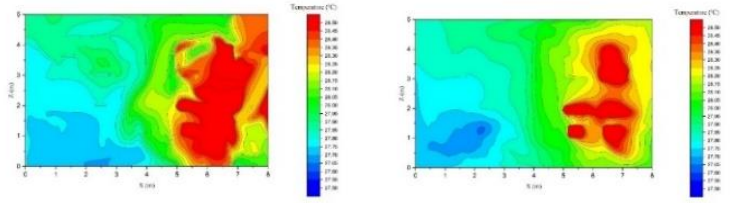

(a) CFD simulation (b) POD interpolation

Fig. 13. The second sub temperature distribution.

After reconstructing each sub temperature field based on the interpolation POD method, the CRI distribution can be calculated according to the Equation (1). The reconstructed CRI is combined with the air temperature collected by the mobile sensor at three locations (A1, A2 and A3) and substituted into the proposed prediction algorithm (Equation (2)) to predict the temperature distribution in the y=1.0m plane. The results are shown in Figure 15.

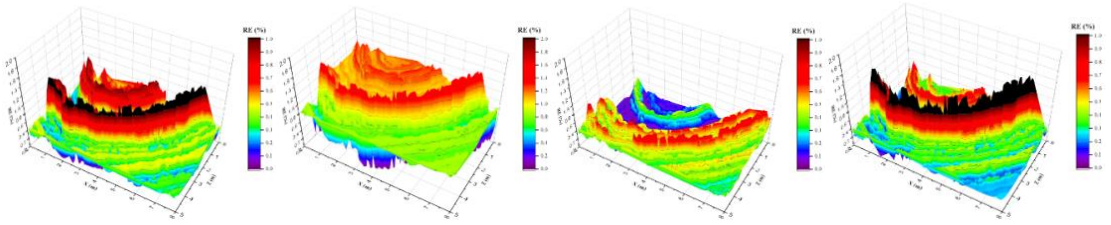

(a) (b) (c) (d)

Fig. 14. Analysis of relative error on y=1.0m plane under different conditions.

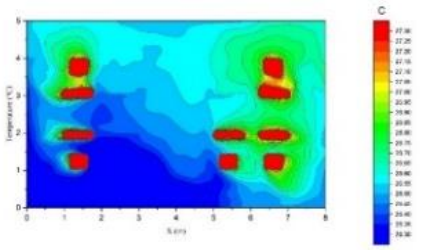

Fig. 15. Prediction results of temperature distribution based on CRI.

Comparing Figure 15 and Figure 11(a), it can be seen that the temperature prediction results in most areas are relatively accurate. Through calculation, in the plane of y=1.0m, the average relative error between the simulation results and the prediction result is 0.57. The detailed relative error analysis is shown in Figure 14(d). From the figure, in most areas, the prediction results are satisfactory. However, the prediction error is relatively large in areas with complex air distribution such as the vicinity of the heat source and the room boundary. The main reasons are as follows: 1) the CRI distribution is obtained based on reconstruction. The impact of airflow distribution has been reflected in the reconstruction process; 2) The following conclusions have also been drawn from previous

study: mobile sensor acquisition points or temperature prediction points are distributed in areas with complex air distribution, which will affect the calculation accuracy of CRI and further affect the prediction accuracy.

4. Published Paper etc.
[Underline the representative researcher and collaborate researchers]
[Published papers]
1. Yanan Zhao, Zihan Zang, Weirong Zhang*, Shen Wei, Yingli Xuan. Predicting indoor temperature distribution based on Contribution Ratio of Indoor Climate (CRI) and mobile sensors. Buildings. 2021, 11(10), 458.
2. Weijia Zhang, Weirong Zhang*, Kunio Mizutani, Haotian Zhang. Decision-makinganalysisofventilationstrategiesunder complex situations: A numerical study [J]. Building and Environment, 2021, 206: 108217.
3. Haotian Zhang, Weirong Zhang*, Weijia Zhang, Yingli Xuan, Yaqi Yue. Multi-vent module-based adaptive ventilation to reduce cross-contamination among indoor occupants[J]. Building and Environment, 2022: 108836.

[Presentations at academic societies]
1. The 11st International Conference on Sustainable Development in the Building and Environment, SuDBE 2021: Application of multi-vent module-based adaptive ventilation (MAV) to improve indoor environment. November 4 to 7, 2021. (Reporter: Weirong Zhang)
2. The 11st International Conference on Sustainable Development in the Building and Environment, SuDBE 2021: Predicting indoor temperature distribution based on contribution ration of indoor climate (CRI) and mobile sensors. November 4 to 7, 2021. (Reporter: Yanan Zhao), Best Academic Report Third Prize
3. The 11st International Conference on Sustainable Development in the Building and Environment, SuDBE 2021: Study on the thermal performance under the implement of multi-vent module-based adaptive ventilation (MAV). November 4 to 7, 2021. (Reporter: Weijia Zhang)
4. The 1st International Workshop on Healthy, Energy Efficiency and Intelligent Building Systems (HEIBS) 2021: Predicting indoor temperature distribution based on contribution ratio of indoor climate (CRI) and mobile sensors. July 12 to 13, 2021 (Reporter: Yanan Zhao)
5. The 1st International Workshop on Healthy, Energy Efficiency and Intelligent Building Systems (HEIBS) 2021: Decision-making analysis of ventilation strategy under complex situations-A numerical study. July 12 to 13, 2021 (Reporter: Weijia Zhang)
6. The 22th China Ventilation Conference 2021: 基于温度移动传感器信息的室内温度分布预测方法. October 21 to 22, 2021 (Reporter: Yanan Zhao)
7. The 22th China Ventilation Conference 2021: 可变动态通风策略对室内热环境的影响研究. October 21 to 22, 2021 (Reporter: Weijia Zhang)
8. The 12th International Symposium on HVAC, ISHVAC 2021: Predicting indoor temperature distribution based on contribution ratio of indoor climate (CRI) and mobile sensors. November 24 to 26, 2021. (Reporter: Yanan Zhao)
9. The 12th International Symposium on HVAC, ISHVAC 2021: Study on the thermal performance under the implement of multi-vent module-based adaptive ventilation (MAV). November 24 to 26, 2021. (Reporter: Weijia Zhang)
10. The 10th Indoor Environment and Health Branch, Chinese Society for Environment Sciences 2021: 基于移动传感器信息的室温分布预测方法. December 3 to 5, 2021. (Reporter: Zihan Zang), Selected as excellent conference paper.

[Published books]
1.
2.

[Other]
Intellectual property rights, Homepage etc.

5. Research Group
1. Representative Researcher
Weirong Zhang, Beijing University of Technology, Professor

2. Collaborate Researchers
1. Yingli Xuan, Tokyo Polytechnic University, Associate Professor
2. Yanan Zhao, Beijing University of Technology, Master Student
3. Weijia Zhang, Beijing University of Technology, Master Student
4. Haotian Zhang, Beijing University of Technology, Master Student
5. Zihan Zang, Beijing University of Technology, Master Student

6. Abstract (half page)

Research Theme: Research on prediction method of indoor temperature distribution based on Contribution Ratio of Indoor Climate (CRI) and mobile sensor information

Representative Researcher (Affiliation): Weirong Zhang (BJUT)

Summary · Figures

Based on the temperature prediction algorithm of CRI and finite air temperature data collected by sensors, this study compares the prediction accuracy of the mobile sensor and the fixed sensor, and explores the effect of different acquisition heights and acquisition intervals of the mobile sensor on the prediction results. Meanwhile, due to the CRI fixed value hypothesis, this study proposes to introduce interpolation POD (proper orthogonal decomposition) method to obtain the dynamic distribution of CRI, so as to improve the prediction accuracy. The effectiveness of the interpolation POD method is verified by an office model. Several conclusions can be drawn from this study:

1) Due to some restrictions in practical applications, using mobile sensors instead of fixed sensors can realize the temperature distribution prediction of residential height on the basis of reducing the number of sensors.
2) The acquisition height of mobile sensors has shown little impact on prediction accuracy in human activity areas and the acquisition distance should be big enough to make the distribution of acquisition points more dispersed.
3) It is effective to introduce the interpolation POD method to reconstruct the sub temperature field and further predict temperature distribution and the prediction error caused by the CRI fixed value hypothesis cannot be ignored.
4) Airflow distribution can have a great impact on results. Therefore, further analysis of the influence of airflow distribution in necessary so as to improve the reconstruction and prediction accuracy.